Progress in Fractional Differentiation and Applications
An International Journal

http://dx.doi.org/10.18576/pfda/120110

Modeling and Mathematical Analysis of the Dynamics of Eye Infection (Conjunctivitis) Virus using Fractal-Fractional and Machine Learning Approach

Mohammed A. El-Shorbagy[1], *Arifa Samreen*[2], *Mati ur Rahman*[3,*] *and Hossam A. Nabwey*[1]

[1] Department of Mathematics, College of Science and Humanities in Al-Kharj, Prince Sattam bin Abdulaziz University, Al-Kharj 11942, Saudi Arabia
[2] Department of Mathematics, National University of Modren Languages Islamabad, Pakistan
[3] Department of Mathematics and Statistics, College of Sciences, Imam Mohammad Ibn Saud Islamic University (IMSIU), Riyadh, Saudi Arabia

Received: 2 Sep. 2025, Revised: 18 Oct. 2025, Accepted: 20 Nov. 2025
Published online: 1 Jan. 2026

Abstract: Mathematical modeling are the key for understanding the diseases transmission within a society. The developed article utilizes the Caputo fractal-fractional operator to examine the dynamics of a mathematical model for viral conjunctivitis infection in the eyes. We presents the existence and uniqueness of the solution for the model under consideration using fixed-point theory. To evaluate the stability of the said system, we uses the Ulam-Hyers (UH) technique. Additionally, we have obtained a numerical solution for the model using fractional Adams-Bashforth iterative methods having predictor and corrector approach. By using the actual numerical values, we examine several options to limit the fractal dimension ξ and the fractional order λ, allowing for an approximation of the model. The application of fractal-fractional calculus has proven effective rule in managing the pandemic and understanding real-world problems. Numerical simulations demonstrate the significance of arbitrary derivative orders, revealing that fractional-fractal orders provide greater insights into the complex dynamics of the proposed conjunctivitis virus model. To illustrate the model dynamics at various fractional orders, several graphical displays are provided. Moreover, a machine learning framework was employed to further assess the effectiveness of the proposed approach in form of neural networking. The obtained results were systematically compared with those generated by the learning model, highlighting both qualitative and quantitative aspects of performance. This comparative analysis revealed that the present method not only provides more accurate and stable solutions having very small small absolute, mean and root mean square errors but also demonstrates improved reliability, thereby confirming its superiority over the machine learning baseline.

Keywords: Adams–Bashforth method; Fractional derivatives; Epidemic model; Qualitative analysis; Numerical simulations; Machine Learning.

1 Introduction, Motivation and Preliminaries

In the early years of the 13^th century, Fibonacci introduced the Fibonacci series for population growth, making it one of the earliest instances of mathematics being used to study biological or social phenomena. Later on, Daniel Bernoulli used mathematical principles to analyze how forces affect the shape of microscopic organisms. In 1901, Johannes Reinke coined the term ”bio math”, thus establishing mathematical biology as a distinct field. Biomathematics essentially explores the fundamental concepts that govern the structure and functions of biological systems through mathematical models. Over the past few decades, there has been a significant increase in the biological sciences and this trend is expected to continue due to major technological advancements. Mathematics has always been a valuable science for society, aiding natural and biological studies [1]. By using mathematical models, we can better understand the complex nature of biology and their biological evaluation.

* Corresponding author e-mail: mrmahman@imamu.edu.sa

The development of computer algebra systems has made it easier to solve complex mathematical problems, allowing researchers to focus on understanding mathematical biology instead of spending time solving puzzles [2]. There is a growing interest in using mathematical models to simulate various biological, physical, and epidemiological phenomena, primarily because these models can incorporate intricate underlying factors. Many individuals are becoming interested in mathematically simulating biological, physical, and epidemiological phenomena. Increasing interest in mathematical models is largely attributed to their ability to incorporate intricate underlying factors. There has been significant interest in mathematical biology from scholars, particularly in areas such as infectious disease modeling, human anatomy growth modeling, body fluid dynamics, and other related fields. Mathematical models have enhanced our comprehension of biological processes and provided fundamental frameworks. Mathematical modeling is crucial for identifying threshold parameters, elucidating transmission dynamics and establishing effective control mechanisms in the context of infectious diseases [3]. Mathematical modeling has been highly effective in the field of infectious diseases, providing practical therapeutic strategies for both treating and preventing viral infections. It serves as an additional tool in combating viral diseases [4].

Red or swollen eyes, also known as conjunctivitis, is a highly infectious disease caused by the inflammation of the conjunctiva. This inflammation can result from bacterial, viral, or allergic infections. Conjunctivitis occurs in different types, with allergic conjunctivitis being common during the pollen season or due to exposure to dust mites, animal dander, or misuse of contact lenses [5,6]. The disease spreads through contact with an affected person who has the infection. This is usually done by coming into contact with discharge from the patient's conjunctiva or upper respiratory tract, or by interacting with objects that have been contaminated by the discharge. Some of the symptoms include redness, watering of the eyes, extreme sensitivity to light, a sore throat, as well as eyelid swelling or pus production. A susceptible person can become infected when they come into contact with an infected carrier. This can happen through contact with discharge from the eyes or upper respiratory secretions of the affected person, or by touching objects that have been contaminated by the hands and then touching the eyes. There is also a risk of direct transmission from mother to baby, especially with chlamydial or gonococcal infections. This discussion will focus on acute hemorrhagic conjunctivitis (AHC), which has an incubation period of 1 to 3 days. Symptoms usually include redness of the eyes, tearing, sensitivity to light, and sometimes a sore throat, along with swollen eyelids or discharge [7]. The illness is more prevalent during the rainy season, as the humidity helps the virus to thrive. Tropical countries such as Thailand see a higher incidence of this illness [8,**?**]. To prevent the spread of the disease, affected individuals should be quarantined. Allowing employees to isolate at home when sick not only speeds up recovery but also reduces the likelihood and duration of spreading the illness to others.

In the context of mathematical modelling, fractional order differential equations offer distinct advantages over ordinary derivatives. A fractional-order model, in conjunction with a delay differential equation model, has been developed for the treatment of the hepatitis C virus using interferon-α (IFN α). This approach is instrumental in elucidating the dynamics of the hepatitis C virus (HCV). It has been empirically demonstrated that the long-term immunological memory, which is crucial for intermediate-range cellular responses, can be effectively represented by a fractional-order derivative [10]. The discrete time delay, denoted as τ, represents the intracellular latency period following an HCV infection before new virions are produced. Time retardation, "t", is used as a bifurcation parameter in the stability analysis of both uninfected and infected states. To further investigate the kinetics of HCV replication in the presence of IFN-α treatment, the authors propose a fractional differential mathematical model that incorporates a uniform non-integer order derivative. The intracellular latency and the interactions between cells inherent to the viral life cycle are thought to reflect fractional-order dynamics [11]. This study examines the dynamical behaviour of hepatitis B during different phases of infection and across multiple transmission events. The authors approach the epidemic issue based on the unique characteristics of the disease [12]. They present a mathematical framework that outlines the effectiveness of tumour vaccination within the context of immunotherapy. The proposed model is governed by fractional-order delay differential equations that include a control variable [13].

Fractional calculus enables the use of derivatives and integrals of non-integer orders, making it highly applicable in various scientific fields, including systems biology. Fractional derivatives and integrals have unique characteristics due to their non-local properties. In the field of epidemiology, diseases such as dysentery are studied using stability theory within the framework of differential equations, which evaluate modeling solutions alongside a combination of control measures. To elucidate the complex issues related to infectious diseases, fractal-fractional mathematical modelling is a crucial component for the study of epidemiology. Among the operators employed in this field are the Atangana-Baleanu and Caputo-Fabrizio derivatives, which are non-local. The Caputo derivative utilises a power-law kernel, while the Caputo-Fabrizio derivative is based on the Mittag-Leffler function of exponential types. Fractional calculus, which finds applications across various disciplines, including physics and engineering, is particularly useful because fractional-order models can effectively capture two significant aspects: genetic dynamics and memory over time [14,**?**].The Mittag-Leffler kernel is used to operationalize a fractal-fractional model of lung cancer growth. This approach enables both qualitative and quantitative analysis of how fractional-order derivatives influence the spread of cancer cells within the human population [14]. A similar development has been made for the coronavirus discovered in 2019: Ahmad et al.

utilize fractional operators to create a model of this virus. They demonstrate the existence and uniqueness of its solutions, as well as the general local stability of the model [15].

To enhance clarity, the authors of the research adopt a three-compartment model to evaluate the effectiveness of vaccines during the ongoing COVID-19 pandemic. This model categorizes individuals into three groups: susceptible, infected, and vaccinated (SIV). They present several graphical representations to illustrate the dynamics of the model, providing context for the space-time variations. Additionally, the analysis employs piecewise equations based on nonsingular Bernoulli convolution using the ABC kernel function [16].The current research examines the poverty outcomes that emerged after the COVID-19 pandemic. To achieve this objective, the authors propose a coupled system of fractional hybrid delay differential equations (FHDDEs) and analyze it using the theory of hybrid fixed points to demonstrate the existence of at least one solution. Their findings indicate that the proposed framework is capable of addressing the factors that worsen the processes of poverty [17]. The current article examines a broad range of sequential fractional differential equations defined using both the Caputo and Atangana-Baleanu definitions of derivatives [18]. Specifically, the authors investigate the necessary conditions and requirements that guarantee the existence of solutions for modified ABC-fractional differential equations (mAB-FDEs) influenced by p-Laplacian nonlinearity [19]. In the fractal-fractional (FF) development of the derivative in individuals with diabetes, the author examines a COVID-19 model [20]. To describe the process of COVID-19 transmission, the author proposes a new mathematical model that incorporates environmental white noise [21].

Additionally, the author presents a stochastic model for the MERS-CoV epidemic [22]. The study also explores two types of operators within an arbitrary nonlinear system of functional differential equations [23]. To explore the dynamics of inadequate testing and diagnosis in models of infectious illnesses, the author substitutes the integer-order derivative with the Caputo operator, utilizing the fractional-order Atangana-Baleanu operator [24]. The author analyzes a discrete Leslie-Gower model that includes a harvesting effect, as well as a Leslie-Gower model featuring a Holling type-IV functional response. This study specifically addresses the interactions within a prey-predator relationship [25]. The author utilizes analysis and statistical methods to investigate resonances and bifurcations within a discrete-time model of prey-predator dynamics [26]. Additionally, the author examines a predator-harvesting predator-prey model in discrete time [27]. Furthermore, the author explores the complex dynamics of a discrete hypothesis regarding the Holling type II functional response in a prey refuge-predator model [28]. The condition is primarily observed during the rainy season, when increased humidity in the air promotes the growth of the virus [29]. It is particularly common in tropical regions [30,**?**], such as Thailand. To prevent the disease from spreading further, it is recommended to isolate those who are affected. Taking sick leave to stay at home and undergo isolation not only leads to a quicker recovery but also minimizes interactions that could be harmful to others [32].

Furthermore, to prevent direct contact among classmates and slow the rapid spread of infections, the American Academy of Pediatrics recommends that adolescents isolate themselves by staying home from school (Davide et al., 2015). Our understanding of conjunctivitis infections has improved due to the development and analysis of mathematical models. Notable studies include those by Chowell et al. (2006) [32], Suksawat and Naowarat (2014) [33], Unyong and Naowarat (2014) [34], and Sangthongjeen et al. (2015) [35]. Additionally, Kulachi et al. (2024) [36] examine non-pharmaceutical approaches for the vaccination, treatment, and early diagnosis of conjunctivitis (eye infection). We studied how conjunctivitis viruses reproduce and infect human eyes, and we developed a new strategy to effectively manage these infections, particularly among both infected and immune populations. The main goal of this document is to create a new mathematical model that includes early detection methods and countermeasures for the conjunctivitis virus, taking into account the effects of treatment or the absence of it.

2 SEVIR model development

Here, the existing model for studying conjunctivitis disease, given in [37], inspires the creation of a new model that incorporates the Caputo fractional operator. To provide a strong historical context, related research types are analyzed and incorporated into the literature. To the best of our knowledge, all previous studies have examined individuals without weakened immune systems, therapy, or vaccinations. We present a novel approach to reducing pink eye infections that combines preventive measures with vaccinations to support immune-compromised patients. To achieve these goals, we have developed a new mathematical model for the conjunctivitis virus. This model includes a sub-population of individuals who are susceptible to conjunctivitis (denoted as $S(t)$) and those who are exposed to the virus (represented by $E(t)$), which is thought to be asymptomatic. The vaccinated individuals who are being monitored for both viral infections and allergic irritants causing pink eye inflammation are indicated by $V(t)$. Additionally, $I(t)$ represents individuals infected with the viral conjunctivitis virus, which spreads throughout the community due to tearing eyes and can be exacerbated by irritants or allergens, often transmitted through hand contamination. Lastly, $R(t)$ stands for individuals who have recovered from both types of conjunctivitis viruses. The parameters involved in the developed system are defined as follows: n represents the total population considered in a specific region. β_n indicates the birth rate relative to the existing

population. μ_n signifies the natural death rate, which applies regardless of infection status. β denotes the transmission rate of the acute hemorrhagic conjunctivitis virus from person to person, particularly when individuals are asymptomatic. Ψ represents the incubation rate during the acute stage, at which point symptoms appear in individuals even after vaccination. $\alpha+\gamma$ symbolizes the incidence rate for recovery, which is influenced by vaccination efforts and robust immune systems. This revised version clarifies the definitions for better understanding. Based on the previously mentioned generalized hypothesis, the model is represented as follows, exhibiting the effect using the novel fractional derivative of order ξ and fractal dimension λ, where $0<\xi\leq 1$

$$\begin{aligned}
{}^{FF}\mathbf{D}_t^{\xi,\lambda}\mathbb{S}(t) &= n\beta_n-\beta I\mathbb{S}-\mu_n\mathbb{S},\\
{}^{FF}\mathbf{D}_t^{\xi,\lambda}\mathbb{E}(t) &= \beta I\mathbb{S}-\phi\mathbb{E}-\mu_n\mathbb{E},\\
{}^{FF}\mathbf{D}_t^{\xi,\lambda}\mathbb{V}(t) &= \phi\mathbb{E}-\kappa\mathbb{V}-\mu_n\mathbb{V},\\
{}^{FF}\mathbf{D}_t^{\xi,\lambda}\mathbb{I}(t) &= \kappa\mathbb{V}-(\alpha+\gamma+\mu_n)\mathbb{I},\\
{}^{FF}\mathbf{D}_t^{\xi,\lambda}\mathbb{R}(t) &= (\alpha+\gamma)\mathbb{I}-\mu_n\mathbb{R}.
\end{aligned} \tag{1}$$

The model is evaluated under the following initial conditions:
$\mathbb{S}(0)=\mathbb{S}_0,\quad \mathbb{E}(0)=\mathbb{E}_0,\quad \mathbb{I}(0)=I_0,\quad \mathbb{R}(0)=\mathbb{R}_i-\mathbb{I}_0.$
The rest of the article we organized is as follows: In Section 1, the formulation of a given mathematical model in the context of fractional calculus has been presented. Section 3 is related to basic definitions and notion of FF derivative. By using fixed point theorems, we show some suitable results for the uniqueness and existence presented in the Section 4. In Section 5, we solve the given model quantitatively using the Adams-Bashforth numerical approach; the numerical findings are also shown and discussed there. Finally, we conclude our work in **??**.

Table 1: **All Quantities and Parameters symbolization**

Symbols	Abbreviations
$\mathbb{S}(t)$	Susceptible to conjunctivitis
$\mathbb{E}(t)$	Exposed to conjunctivitis
$\mathbb{V}(t)$	Vaccinated individuals for both viral and allergic infections
$\mathbb{I}(t)$	Infected with the viral conjunctivitis virus
$\mathbb{R}(t)$	Recovered from both types of conjunctivitis viruses
n	Total population in specific region
β_n	Birth rate relative to the existing population
μ_n	Natural death rate
β	Transmission rate of the acute hemorrhagic conjunctivitis virus
Ψ	Incubation rate during the acute stage
$\alpha+\gamma$	incidence rates for recovery

3 Preliminaries

Definition 1.*[38] Let $\mathscr{U}(t)$ on $a<t<b$, be a continuous and differentiable function with fractional order ξ and fractal dimension λ, then the FF order derivative can be defined as*

$${}^{FF}\mathbf{D}_t^{\xi,\lambda}(\mathscr{U}(t))=\frac{1}{(p-\xi)}\frac{d}{dt^{\lambda}}\int_0^t(t-y)^{p-\xi-1}\mathscr{U}(y)dy, \tag{2}$$

along-with $p-1<\xi$, $\lambda\leq p$, where $p\in\mathbb{N}$ and $\frac{d\mathscr{U}(y)}{dy^{\lambda}}=\lim_{t\to 0}\frac{\mathscr{U}(t)-\mathscr{U}(y)}{t^{\lambda}-y^{\lambda}}$

Definition 2.*[38] Let $\mathscr{U}(t)$ be continuous on $a<t<b$ then the FF order integral of $\mathscr{U}(t)$ with fractional order ξ and fractal dimension λ is defined as*

$${}^{FF}\mathbf{I}^{\xi}\mathscr{U}(t)=\frac{\lambda}{\Gamma(\xi)}\int_0^t(t-y)^{\xi-1}y^{\lambda-1}\mathscr{U}(y)dy. \tag{3}$$

Definition 3.*The system (1) is UH stable if $\exists$ any real number $\mathscr{B}_{\xi,\lambda}\geq 0$ such that $\forall\ \varepsilon>0$ and all the solutions $\Omega\in C^1(\mathscr{X},\mathbb{R})$, the inequality can be defined as*

$$|{}^{FF}\mathbf{D}^{\xi,\lambda}\Omega(\mathrm{t})-\Phi(t,\Omega(t))|\leq\varepsilon,\quad t\in\mathscr{X},$$

$\mathscr{Y} \in C^1(\mathscr{X}, \mathbb{R})$ is the unique solution for the considered model (1), such that

$$|\Omega(t) - \mathscr{Y}(t)| \leq \mathscr{B}_{\xi,\lambda}, \quad t \in \mathscr{X},$$

Note:. In order to conduct a thorough qualitative analysis, we will construct a Banach space. $\mathrm{U} = \mathrm{X} \times \mathrm{X} \times \mathrm{X} \times \mathrm{X} \times \mathrm{X}$ where $\mathrm{X} = \mathscr{B}(\mathscr{X})$ with norm: $\|\Omega\| = \|\mathbb{S}, \mathbb{E}, \mathbb{V}, \mathbb{I}, \mathbb{R}\| = \max_{t\in[0,T]}\{|\mathbb{S}(t)| + |\mathbb{E}(t)| + |\mathbb{V}(t)| + |\mathbb{I}(t)| + |\mathbb{R}(t)|\}$.

3.1 Positivity and boundedness of solutions

Here, we demonstrate the positivity and boundedness of the constructed system. Let $\Xi(t) = \{\mathbb{S}, \mathbb{E}, \mathbb{V}, \mathbb{I}, \mathbb{R}\} \in \mathbf{R}^5_+$. We need the following theorem to prove the positivity of the solution:

Theorem 31*The region $\mathbf{R}^5_+$ is positively invariant, and the remaining solution remains bounded throughout this region.*

*Proof.*The results of the system presented in equation (1) are shown below, highlighting the positive solution:

$$\begin{aligned}
{}^{FF}\mathbf{D}^{\xi,\lambda}\mathbb{S}(t)\big|_{\mathbb{S}=0} &= n\beta_n \geqslant 0,\\
{}^{FF}\mathbf{D}^{\xi,\lambda}\mathbb{E}(t)\big|_{\mathbb{V}=0} &= \beta\mathbb{I} \geqslant 0,\\
{}^{FF}\mathbf{D}^{\xi,\lambda}\mathbb{V}(t)\big|_{\mathbb{I}=0} &= \phi\mathbb{E} \geqslant 0,\\
{}^{FF}\mathbf{D}^{\xi,\lambda}\mathbb{I}(t)\big|_{\mathbb{R}=0} &= \kappa\mathbb{V} \geqslant 0,\\
{}^{FF}\mathbf{D}^{\xi,\lambda}\mathbb{R}(t)\big|_{\mathbb{M}=0} &= (\alpha+\gamma)\mathbb{I} \geqslant 0.
\end{aligned} \tag{4}$$

According to the aforementioned system, $\mathbf{R}^5_+$ presents the model solution for $t \geqslant 0$. By summing all equations in (1), and assuming that $X = \mathbb{S} + \mathbb{E} + \mathbb{V}$, we obtain

$${}^{FF}\mathbf{D}^{\xi,\lambda}X = n\beta_n - \kappa V - \mu_n(\mathbb{S} + \mathbb{E} + \mathbb{V}),$$

$$= n\beta_n - \kappa V - \mu_n X.$$

$$\Lambda^1_v = \left\{\mathbb{S}, \mathbb{E}, \mathbb{V} \in \mathbb{R}^3_+ \,\middle|\, \mathbb{S} + \mathbb{V} \leq X\right\}, \quad \forall t \geq 0$$

and If we consider $X_v = \mathbb{I} + \mathbb{R}$. Therefore, we have developed

$${}^{FF}\mathbf{D}^{\xi,\lambda}X_v(t) = \kappa V - \mu_n(\mathbb{I} + \mathbb{R}),$$

$$= \kappa V - \mu_n X_v.$$

Taking $t \to \infty$, and after solving, we get:

$$X_v \leq \frac{\kappa V}{\mu_n}.$$

Thus,

$$\Lambda^1_v = \left\{\mathbb{I}, \mathbb{R} \in \mathbb{R}^2_+ \mid X_v \leq \frac{\kappa V}{\mu_n}\right\}, \quad \forall t \geq 0.$$

Consequently, the feasible region of the system (1) can be defined as

$$\Lambda^1 = \left\{\mathbb{S} + \mathbb{E} + \mathbb{V} + \mathbb{I} + \mathbb{R} \in \mathbb{R}^5_+ \,\middle|\, S + V \leq X,\, X\nu \leq \frac{\kappa V}{\mu_n}\right\}, \quad \forall t \geq 0$$

.

4 Existence of a solution for the fractional order Eye infection conjunctivitis virus model

The analytical framework (4) exhibits both nonlinear properties and nonlocal characteristics. The mathematical model requires exact solutions that no particular procedures or methods can discover. Solution existence demonstrates that specific conditions enable researchers to discover exact solutions. Here we explore whether solutions exist in the proposed model by applying fixed-point theorem analysis. Since the given integral is differentiable, so we can express the RHS of the model (4) as fallows

$$\begin{aligned}
{}^{\mathscr{R}\mathscr{L}}\mathbf{D}^{\xi}\mathbb{S}(t) &= \lambda t^{\lambda-1}\mathsf{W}_1(\mathbb{S},\mathbb{E},\mathbb{V},\mathbb{I},\mathbb{R},t) = n\beta_n - \beta I\mathbb{S} - \mu_n\mathbb{S},\\
{}^{\mathscr{R}\mathscr{L}}\mathbf{D}^{\xi}\mathbb{E}(t) &= \lambda t^{\lambda-1}\mathsf{W}_2(\mathbb{S},\mathbb{E},\mathbb{V},\mathbb{I},\mathbb{R},t) = \beta I\mathbb{S} - \phi\mathbb{E} - \mu_n\mathbb{E},\\
{}^{\mathscr{R}\mathscr{L}}\mathbf{D}^{\xi}\mathbb{V}(t) &= \lambda t^{\lambda-1}\mathsf{W}_3(\mathbb{S},\mathbb{E},\mathbb{V},\mathbb{I},\mathbb{R},t) = \phi\mathbb{E} - \kappa\mathbb{V} - \mu_n\mathbb{V},\\
{}^{\mathscr{R}\mathscr{L}}\mathbf{D}^{\xi}\mathbb{R}(t) &= \lambda t^{\lambda-1}\mathsf{W}_5(\mathbb{S},\mathbb{E},\mathbb{V},\mathbb{I},\mathbb{R},t) = \kappa\mathbb{V} - (\alpha+\gamma+\mu_n)\mathbb{I},\\
{}^{\mathscr{R}\mathscr{L}}\mathbf{D}^{\xi}\mathbb{I}(t) &= \lambda t^{\lambda-1}\mathsf{W}_6(\mathbb{S},\mathbb{E},\mathbb{V},\mathbb{I},\mathbb{R},t) = (\alpha+\gamma)\mathbb{I} - \mu_n\mathbb{R}.
\end{aligned} \tag{5}$$

The development methodology for the advanced model at (5) uses the following structure to evaluate $t \in \mathscr{X}$.

$$\begin{aligned}
{}^{\mathscr{R}\mathscr{L}}\mathbf{D}^{\xi}\Omega(\mathsf{t}) &= \lambda t^{\lambda-1}\Phi(\mathsf{t},\Omega(\mathsf{t})), \quad 0<\xi,\lambda\le 1,\\
\Omega(0) &= \Omega_0,
\end{aligned} \tag{6}$$

we will solve equation (6) by replacing ${}^{\mathscr{R}\mathscr{L}}\mathbf{D}^{\xi,\lambda}$ with ${}^{\mathscr{C}}\mathbf{D}^{\xi,\lambda}$ while using Riemann-Liouville integration:

$$\Omega(\mathsf{t}) = \Omega_0(\mathsf{t}) + \frac{\eta}{\Gamma(\xi)}\int_0^t y^{\eta-1}(t-y)^{\xi-1}\Phi(y,\Omega(y))dy, \tag{7}$$

where

$$\begin{cases}
\Omega(t) = (\mathbb{S}(t),\mathbb{E}(t),\mathbb{V}(t),\mathbb{I}(t),\mathbb{R}(t))^T,\\
\Omega_0(t) = (\mathbb{S}(0),\mathbb{E}(0),\mathbb{V}(0),\mathbb{I}(0),\mathbb{R}(0))^T,\\
\Phi(t,\Omega(t)) = (\mathsf{W}_i(\mathbb{S},\mathbb{E},\mathbb{V},\mathbb{I},\mathbb{R},t))^T,\ \ i=1,2,...5.
\end{cases} \tag{8}$$

We will now define the operator and transform Eq. (4) into a fixed point problem. $\mathscr{T}:\mathbf{Q}\to\mathbf{Q}$

$$\mathscr{T}(\Omega)(\mathsf{t}) = \Omega_0(\mathsf{t}) + \frac{\eta}{\Gamma(\xi)}\int_0^t y^{\eta-1}(t-y)^{\xi-1}\Phi(y,\Omega(y))dy. \tag{9}$$

The outcomes demonstrating the existence of the model are based on the theorem presented in reference [39].

Theorem 41 *Consider the operator $\mathscr{T}:\mathbf{Q}\to\mathbf{Q}$. A fully continuous mapping can therefore be described as follows:*

$$\mathscr{J}(\mathscr{T}) = \{\Omega\in\mathbf{Q}:\Omega=\tau\mathscr{T}(\Omega),\tau\in[0,1]\},$$

is bounded then the operator $\mathscr{T}$ possesses at least one fixed point within the $\mathbf{Q}$.

Proof. The proof is given in the next theorem.

In the below theorem the fractal fractional integration is mostly converted to beta function $\mathrm{B}(\xi,\lambda)$

Theorem 42 *The operator $\mathscr{T}$ is considered "compact", if the operator $\Phi:\mathscr{D}\times\mathbf{Q}\to\mathbb{R}$ preserves continuity.*

Proof. The mathematical transformation $\mathscr{T}:\mathbf{Q}\to\mathbf{Q}$, as defined by equation (9), will be demonstrated to be continuous. The set $\mathscr{P}$, which belongs to $\mathbf{Q}$, demonstrates boundedness. This condition necessitates the existence of a constant $\mathscr{C}_\Psi>0$ for each element $\Omega\in\mathscr{P}$ such that $|\Phi(t,\Omega(t))|\le\mathscr{C}_\Psi$ holds simultaneously. Moreover, for all $\Omega\in\mathscr{P}$, we have

$$\begin{aligned}
\|\mathscr{T}(\Omega)\| &\le \frac{\eta\mathscr{C}_\Phi}{\Gamma(\xi)}\max_{t\in[0,T]}\left|\int_0^t(\tau-y)^{\xi-1}y^{\eta-1}dy\right|\\
&\le \frac{\eta\mathscr{C}_\Phi}{\Gamma(\xi)}\max_{t\in[0,T]}\int_0^t(1-z)^{\lambda-1}z^{\xi-1}t^{\xi+\lambda-1}dz\\
&\le \frac{\eta\mathscr{C}_\Phi T^{\xi+\lambda-1}}{\Gamma(\xi)}\mathrm{B}(\xi,\lambda),
\end{aligned} \tag{10}$$

the operator $\mathscr{T}$ exhibits uniform boundedness as stated in Eq. (10), which involves the Beta function $\mathrm{B}(\xi,\lambda)$. Additionally, the operator $\mathscr{T}$ demonstrates the property of equi-continuity for $t_1, t_2 \in \mathscr{D}$ and $\Omega \in \mathscr{P}$ described as

$$\begin{aligned}\|\mathscr{T}(\Omega(t_1)) - \mathscr{T}(\Omega(t_2))\| &\leq \frac{\eta \mathscr{C}_\Phi}{\Gamma(\xi)} \max_{t\in[0,T]} \left| \int_0^{t_1} (t_1-y)^{\xi-1} y^{\lambda-1} dy - \int_0^{t_2} (t_2-y)^{\xi-1} y^{\lambda-1} dy \right| \\ &\leq \frac{\eta \mathscr{C}_\Phi \mathrm{B}(\xi,\lambda)}{\Gamma(\xi)} (t_1^{\xi+\lambda-1} - t_2^{\xi+\lambda-1}) \to 0 \quad as \quad t_1 \to t_2.\end{aligned}$$

Consequently, the operator $\mathscr{T}$ is characterized by equi-continuity. The application of the Arzelà-Ascoli theorem confirms that $\mathscr{T}$ is bounded, due to its continuity as well as its properties of complete continuity and compactness.

Furthermore, we are operating under the following hypothesis:

(i)$\exists$ constants $\mathrm{A}_\Phi > 0 \ni$ for each $\Omega,\ \bar{\Omega} \in \mathrm{f}$ we have

$$|\Phi(t,\Omega) - \Phi(t,\bar{\Omega})| \leq \mathrm{A}_\Phi |\Omega| - |\bar{\Omega}|.$$

The proof regarding the existence and uniqueness of solutions is derived using the fixed point method as described by Granas *et al.* [39].

Theorem 43*The model presented in equation* (4) *exhibits a unique solution under the conditions specified in hypothesis* (**i**)*, provided that the parameter* λ *is less than 1 is given by*

$$\lambda = \frac{\lambda \mathrm{A}_\Phi \mathrm{T}^{\xi+\lambda-1}}{\Gamma(\xi)} \mathrm{B}(\xi,\lambda) \tag{11}$$

*Proof.*Let us assume, $\max_{t\in[0,T]} |\Phi(t,0)| = \mathscr{K}_\Phi < \infty$, such that

$$r \geq \frac{\eta \mathrm{T}^{\xi+\lambda-1} \mathrm{B}(\xi,\lambda) \mathscr{K}_\Phi}{\Gamma(\xi) - \lambda \mathrm{T}^{\xi+\lambda-1} \mathrm{B}(\xi,\lambda) \mathrm{A}_\Phi}. \tag{12}$$

It has been proven $\mathscr{T}(\mathscr{P}_r) \subset \mathscr{P}_r$, where $\mathscr{P}_r = \{\Omega \in \mathrm{f} : \|\Omega\| \leq r\}$ and $\Omega \in \mathscr{P}_r$, we have

$$\begin{aligned}\|\mathscr{T}(\Omega)\| &\leq \frac{\eta}{\Gamma(\xi)} \max_{t\in[0,T]} \int_0^t y^{\eta-1}(t-y)^{\xi-1} \big(|\Phi(t,\Omega(t)) - \Phi(t,0)| + |\Phi(t,0)|\big) dy \\ &\leq \frac{\eta \mathrm{T}^{\beta+\lambda-1} \mathrm{B}(\beta,\lambda)(\mathrm{A}_\Phi \|\Omega\| + \mathscr{K}_\Phi)}{\Gamma(\beta)}, \\ &\leq \frac{\eta \mathrm{T}^{\beta+\eta-1} \mathrm{B}(\beta,\lambda)(\mathrm{A}_\Phi r + \mathscr{K}_\Phi)}{\Gamma(\beta)}, \\ &\leq r.\end{aligned}$$

Assume that the operator $\mathscr{T} : \mathbf{Q} \to \mathbf{Q}$ is given by equation (9). Under the assumption that $\mathbf{C}$ exists, we obtain $t \in \mathscr{D}$, Ω, and $\overline{\mathscr{W}} \in \mathscr{D}$ for each instance. Suppose the operator $\mathscr{T} : \mathbf{Q} \to \mathbf{Q}$ is defined as in (9). Using the assumption $\mathbf{C}$ and for every $t \in \mathscr{D}$, Ω, $\overline{\mathscr{W}} \in \mathscr{D}$, we obtain

$$\begin{aligned}\|\mathscr{T}(\Omega) - \mathscr{T}(\overline{\mathscr{W}})\| &\leq \frac{\eta}{\Gamma(\xi)} \max_{t\in[0,T]} \left| \int_0^t y^{\lambda-1}(t-y)^{\beta-1} \Phi(y,\Omega(y)) dy - \int_0^t y^{\lambda-1}(t-y)^{\xi-1} \Phi(y,\overline{\Omega}(y)) dy \right|, \\ &\leq \xi \|\Omega - \bar{\mathscr{W}}\| \end{aligned} \tag{13}$$

Equation (13) is used to make the operator $\mathscr{T}$ a contraction. Since there is only one solution to equation (7), our model (4) must also have a unique solution.

In addressing the system outlined by (4), it is essential to establish UH stability by considering $\phi \in C(\mathscr{D})$ and examining the solution where $\phi(0) = 0$. Subsequently,

– $|\psi(t)| \leq \varepsilon$, for $\varepsilon > 0$;
– ${}^{FF}\mathrm{D}_t^{\xi,\lambda} \Omega(t) = \Phi((t),\Omega(t)) + \psi(t)$.

Lemma 1.*The solution of perturbed equation*

$$
\begin{aligned}
{}^{FF}\mathbf{D}^{\xi,\lambda}\Omega(t) &= \Phi(t,\Omega((t))+\psi(t),\\
\Omega(0) &= \Omega_0
\end{aligned}
\tag{14}
$$

satisfies the given relationship

$$
\begin{aligned}
\left|\Omega(t)-\left(\Omega_0(t)+\frac{\lambda}{\Gamma(\xi)}\int_0^t y^{\lambda-1}(t-y)^{\xi-1}\Phi(y,\Omega(y))\right)\right| &\leq \left(\frac{\lambda \mathrm{T}^{\xi+\lambda-1}\mathrm{B}(\xi,\lambda)}{\Gamma(\xi)}\right)\varepsilon\\
&= \mathrm{C}_{\xi,\lambda}\varepsilon.
\end{aligned}
\tag{15}
$$

Theorem 44*It has been established that the integral solution of* (4) *is UH stable according to* (**C**) *and* (15)*. Therefore, if* $\eta < 1$*, as defined in* (11)*, the model's analytical conclusions remain UH stable.*

*Proof.*Assuming that $\mathrm{Z} \in \mathbf{Q}$ represents the unique solution to equation (7), and $\Omega \in \mathbf{Q}$ denotes any solution to the same equation, we can derive equation (2) through the application of fractal-fractional integration

$$
\begin{aligned}
|\Omega(t)-\mathrm{Z}(t)| &= \left|\Omega(t)-\left(\mathrm{Z}_0(t)+\frac{\lambda}{\Gamma(\xi)}\int_0^t (t-y)^{\xi-1}y^{\lambda-1}\Phi(y,\mathrm{Z}(y))dy\right)\right|,\\
&\leq \left|\Omega(t)-\left(\Omega_0(t)+\frac{\lambda}{\Gamma(\xi)}\int_0^t (t-y)^{\xi-1}y^{\lambda-1}\Phi(y,\Omega(y))dy\right)\right|,\\
&+ \left|\left(\Omega_0(t)+\frac{\eta}{\Gamma(\beta)}\int_0^t (t-y)^{\beta-1}y^{\eta-1}\Phi(y,\omega(y))dy\right)\right.\\
&- \left.\left(\mathrm{Z}_0(t)+\frac{\eta}{\Gamma(\beta)}\int_0^t (t-y)^{\beta-1}y^{\eta-1}\Phi(y,\mathrm{Z}(y))dy\right)\right|,\\
&\leq \mathrm{C}_{\beta,\eta}\varepsilon+\frac{\eta \mathrm{T}^{\beta+\eta-1}\mathrm{L}_\omega}{\Gamma(\beta)}\mathrm{B}(\beta,\eta)\|\omega-\mathrm{Z}\|,\\
&\leq \mathrm{C}_{\beta,\eta}+\eta\|\omega-\mathrm{Z}\|.
\end{aligned}
$$

Which we have

$$
\|\Omega-\mathrm{Z}\| \leq \mathrm{C}_{\xi,\lambda}+\eta\|\omega-\mathrm{Z}\|,
\tag{16}
$$

referring to equation (16), we can express it as

$$
\|\Omega-\mathrm{Z}\| \leq \left(\frac{\mathrm{C}_{\xi,\lambda}}{1-\lambda}\right)\varepsilon.
\tag{17}
$$

Thus, we conclude that the solution of (7) is UH stable according to Equation (17). Consequently, the solution of (4) in the proposed model is also UH stable.

5 Numerical Scheme

In this section of the manuscript, we will outline a numerical approach to simulate the system under consideration. We will numerically simulate Equation (7) using the fractional Adams-Bashforth technique [40]. The method applied the predictor corrector approach. Our analysis will focus on the system defined by (4).

$$
\begin{aligned}
{}^{FF}\mathbf{D}_t^{\xi,\lambda}\mathbb{S}(t) &= \mathsf{G}_1(\mathbb{S},t) = n\beta_n-\beta I\mathbb{S}-\mu_n\mathbb{S},\\
{}^{FF}\mathbf{D}_t^{\xi,\lambda}\mathbb{E}(t) &= \mathsf{G}_2(\mathbb{E},t) = \beta I\mathbb{S}-\phi\mathbb{E}-\mu_n\mathbb{E},\\
{}^{FF}\mathbf{D}_t^{\xi,\lambda}\mathbb{V}(t) &= \mathsf{G}_3(\mathbb{V},t) = \phi\mathbb{E}-\kappa\mathbb{V}-\mu_n\mathbb{V},\\
{}^{FF}\mathbf{D}_t^{\xi,\lambda}\mathbb{I}(t) &= \mathsf{G}_4(\mathbb{I},t) = \kappa\mathbb{V}-(\alpha+\gamma+\mu_n)\mathbb{I},\\
{}^{FF}\mathbf{D}_t^{\xi,\lambda}\mathbb{R}(t) &= \mathsf{G}_5(\mathbb{R},t) = (\alpha+\gamma)\mathbb{I}-\mu_n\mathbb{R}.
\end{aligned}
\tag{18}
$$

Applying the definitions of fractal fractional integration as given in equation 7 yields the following relationship:

$$\begin{aligned}
\mathbb{S}(t) &= \mathbb{S}(0) + \frac{\lambda}{\Gamma(\xi)} \int_0^t x^{\lambda-1}(t-y)^{\xi-1} \mathsf{G}_1(\mathbb{S},y)dy,\\
\mathbb{E}(t) &= \mathbb{E}(0) + \frac{\lambda}{\Gamma(\xi)} \int_0^t x^{\lambda-1}(t-y)^{\xi-1} \mathsf{G}_2(\mathbb{E},y)dy,\\
\mathbb{V}(t) &= \mathbb{V}(0) + \frac{\lambda}{\Gamma(\xi)} \int_0^t x^{\lambda-1}(t-y)^{\xi-1} \mathsf{G}_3(\mathbb{V},y)dy,\\
\mathbb{I}(t) &= \mathbb{I}(0) + \frac{\lambda}{\Gamma(\xi)} \int_0^t x^{\lambda-1}(t-y)^{\xi-1} \mathsf{G}_4(\mathbb{I},y)dy,\\
\mathbb{R}(t) &= \mathbb{R}(0) + \frac{\lambda}{\Gamma(\xi)} \int_0^t x^{\lambda-1}(t-y)^{\xi-1} \mathsf{G}_5(\mathbb{R},y)dy.
\end{aligned} \tag{19}$$

We will now utilize the newly discovered t_{k+1} technique to numerically solve equation (19). Thus, the initial equation of the system is:

$$\mathbb{S}_{(k+1)} = \mathbb{S}(0) + \frac{\lambda}{\Gamma(\xi)} \int_0^{t_{k+1}} y^{-1}(t_{k+1}-y)^{\xi-1} \mathsf{G}_1(\mathbb{S},y)dy$$

Over the infinite interval $[t_\tau, t_{\tau+1}]$, the function $\mathsf{G}_1(\mathbb{S},y)$, expressed in terms of Lagrange interpolation polynomials, along with $= t_\tau - t_{\tau-1}$, can be represented as follows:

$$\mathbb{S}_{(k)} \approx \frac{1}{} \left[(t-t_{\tau-1}) t_\tau^{\lambda-1} \mathsf{G}_1(\mathbb{S}_{(\tau)}, t_\tau) - (t-t_\tau) t_{\tau-1}^{\lambda-1} \mathsf{G}_1(\mathbb{S}_{(\tau-1)}, t_{\tau-1}) \right], \tag{20}$$

After changing (20) to (20), we can rewrite (20) as

$$\mathbb{S}_{(k+1)} = \mathbb{S}(0) + \frac{\lambda}{\Gamma(\xi)} \sum_{j=0}^{k} \int_{t_j}^{t_{j+1}} y^{\lambda-1}(t_{k+1}-y)^{\xi-1} \mathbb{S}_k dy. \tag{21}$$

The numerical iterative findings for the $\mathbb{S}$ class, as stated in (4), are obtained by employing the FF derivatives in the Caputo form to simplify the integrals on the right side of (21):

$$\begin{aligned}
\mathbb{S}_{(k+1)} = \mathbb{S}(0) &+ \frac{\lambda^\xi}{\Gamma(\xi+2)} \sum_{\tau=0}^{k} \left[t_\tau^{\lambda-1} \mathsf{G}_1(\mathbb{S}_{(\tau)}, t_\tau) \right.\\
&\times \Big((k+1-\tau)^\lambda (k-\tau+2+\lambda) - (k-\tau)^\lambda (k-\tau+2+2\lambda) \Big)\\
&\left. - t_{\tau-1}^{\lambda-1} \mathsf{G}_1(\mathbb{S}_{(\tau-1)}, t_{\tau-1}) \Big((k+1-\tau)^\lambda + 1 - (k-\tau)^\lambda (k-\tau+1+\lambda) \Big) \right],
\end{aligned} \tag{22}$$

Similarly, the remaining terms could be written as

$$\begin{aligned}
\mathbb{E}_{(k+1)} = \mathbb{E}(0) &+ \frac{\lambda^\xi}{\Gamma(\xi+2)} \sum_{\tau=0}^{k} \left[t_\tau^{\lambda-1} \mathsf{G}_2(\mathbb{E}_{(\tau)}, t_\tau) \right.\\
&\times \Big((k+1-\tau)^\lambda (k-\tau+2+\lambda) - (k-\tau)^\lambda (k-\tau+2+2\lambda) \Big)\\
&\left. - t_{\tau-1}^{\lambda-1} \mathsf{G}_2(\mathbb{E}_{(\tau-1)}, t_{\tau-1}) \Big((k+1-\tau)^\lambda + 1 - (k-\tau)^\lambda (k-\tau+1+\lambda) \Big) \right],
\end{aligned} \tag{23}$$

$$\begin{aligned}
\mathbb{V}_{(k+1)} = \mathbb{V}(0) &+ \frac{\lambda^\xi}{\Gamma(\xi+2)} \sum_{\tau=0}^{k} \left[t_\tau^{\lambda-1} \mathsf{G}_3(\mathbb{V}_{(\tau)}, t_\tau) \right.\\
&\times \Big((k+1-\tau)^\lambda (k-\tau+2+\lambda) - (k-\tau)^\lambda (k-\tau+2+2\lambda) \Big)\\
&\left. - t_{\tau-1}^{\lambda-1} \mathsf{G}_3(\mathbb{V}_{(\tau-1)}, t_{\tau-1}) \Big((k+1-\tau)^\lambda + 1 - (k-\tau)^\lambda (k-\tau+1+\lambda) \Big) \right],
\end{aligned} \tag{24}$$

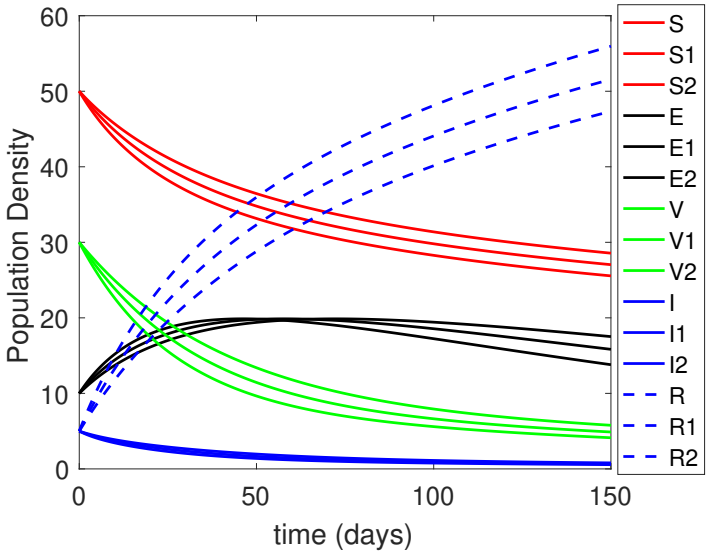

Fig. 1: Combined dynamics of all five compartments on three different fractal dimensions and fractional orders.

$$\mathbb{I}_{(k+1)} = \mathbb{I}(0) + \frac{\lambda^{\xi}}{\Gamma(\xi+2)} \sum_{\tau=0}^{k} \Bigg[t_{\tau}^{\lambda-1} \mathsf{G}_4(\mathbb{I}_{(\tau)}, t_{\tau}) \times \Big((k+1-\tau)^{\lambda}(k-\tau+2+\lambda) - (k-\tau)^{\lambda}(k-\tau+2+2\lambda) \Big) - t_{\tau-1}^{\lambda-1} \mathsf{G}_4(\mathbb{I}_{(\tau-1)}, t_{\tau-1}) \Big((k+1-\tau)^{\lambda} + 1 - (k-\tau)^{\lambda}(k-\tau+1+\lambda) \Big) \Bigg], \tag{25}$$

$$\mathbb{R}_{(k+1)} = \mathbb{R}(0) + \frac{\lambda^{\xi}}{\Gamma(\xi+2)} \sum_{\tau=0}^{k} \Bigg[t_{\tau}^{\lambda-1} \mathsf{G}_5(\mathbb{R}_{(\tau)}, t_{\tau}) \times \Big((k+1-\tau)^{\lambda}(k-\tau+2+\lambda) - (k-\tau)^{\lambda}(k-\tau+2+2\lambda) \Big) - t_{\tau-1}^{\lambda-1} \mathsf{G}_5(\mathbb{R}_{(\tau-1)}, t_{\tau-1}) \Big((k+1-\tau)^{\lambda} + 1 - (k-\tau)^{\lambda}(k-\tau+1+\lambda) \Big) \Bigg], \tag{26}$$

5.1 Numerical simulation and Discussion

In this section we simulate the said fractal fractional model by using the technique of Adams-bashforth scheme using the data taken from [41]. The initial conditions for all classes in the form of populations are $\mathbb{S}_0 = 50, \mathbb{E}_0 = 10, \mathbb{V}_0 = 30, \mathbb{I}_0 = 5, \mathbb{R}_0 = 5$, along with fractal dimension $\xi = 0.6, 0.8, 1$ and fractional order $\lambda = 0.6, 0.8, 1$ respectively. The used parameters are $n = 100, \beta_n = 0.00004215, \mu_n = 0.00004215, \beta = 0.004, \alpha = 0.08, \gamma = 0.33, \phi = 0.01, \kappa = 0.04$.

The graphical representation of all five compartments are given in Figures 1 and 2 by using the algorithm of Adams-Bahforth technique on fractal (ξ) fractional (λ) orders and integer order respectively. The number of susceptible peoples are slightly declines when they are exposed to the eye infection but with inclusion of vaccination the expose and infected class recovered and will shift to the normal healthy class. The complex geometry of the eye allergy model are described best by the fractal and fractional concept with different fractional orders lying between 0 and 1. The recovery from the infection are achieved quickly on small fractal dimensions and fractional orders. The integer dynamics with slow recovery is shown in figure 2 on fractal fractional order of 1.

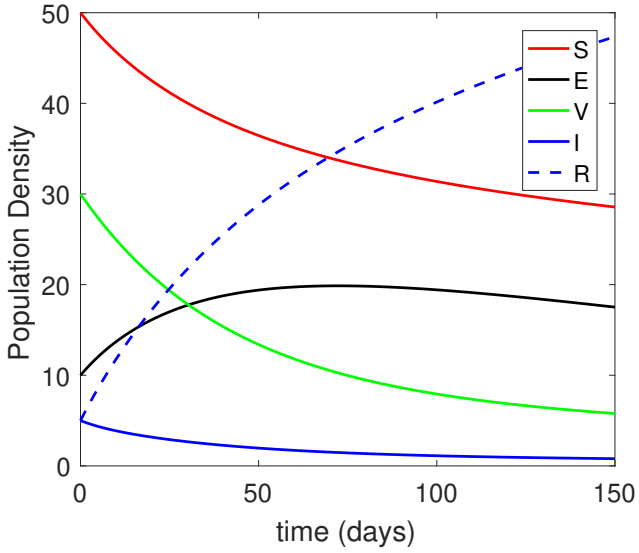

Fig. 2: Combined dynamics of all five compartments on three different fractal dimensions and fractional orders.

5.2 Neural Network dynamics

In this section the used data are examined by neural network (NN) analysis composed of convolution of different hidden layers like stochastic form for 1000 iterations. The comparison with exact solution through Adams–Bashforth–Moulton technique to the simulated solution through neural network is given in figure **??**. Both are overlapped on each other showing with small errors in all compartments. Further, the fractal dimensions and fractional analysis gives more information related to the said dynamics with extra data of ξ, λ for complex geometry. The Plot **??** represents the absolute error for all agents of the fractal fractional order eye infection dynamical model.

Figure **??** shows the examination of all data for the given model in fractal-fractional format by deep NN with 1 coefficient of regression being fitted well. The mean square error (MSE) is 7.8×10^{-06} and the root mean square error (RMSE) is 2.7×10^{-03}. The mean and variance errors are -6.2×10^{-05} and 2.7×10^{-03} in histogram format. The small error implies correctness of the obtained scheme. Figure **??** tested train data in fractal-fractional form for the said model with regression 1, the MSE is $8.2 \times 10^{-06}$and RMSE is 2.8×10^{-03} while the mean error is 1.02×10^{-06} and variance error is 2.8×10^{-03} in the histogram plot. Figure **??** showsthe graphical representation for valid data in fractal-fractional form for the said model with regression is 1, the MSE is $6 \times 10^{-06}$and RMSE is 2.4×10^{-03} while the mean error is -1.1×10^{-04} and variance error is 2.4×10^{-03} in the histogram plot. Figure **??** shows test data in fractal-fractional format for the given model with regression is 1, the MSE is 7.7×10^{-06} and RMSE is 2.7×10^{-03} while the mean error is -3.0×10^{-03} and variance error is 2.7×10^{-03} in the histogram plot showing best accuracy.

Furthermore the graphical representations of the performance for train, valid and test data for all five compartments in fractal fractional formate on 1000 epoch is 2.9974×10^{-08} shown in figure **??**. Next the error of all compartments for 20 bins of train, valid and test data are given in figure **??**. The target for regression of data and fitting in the form of output =Target$+ \times +2.4 \times 10^{e} - 07$ for train data, output =Target $+ \times +2.7 \times 10^{e} - 05$ for valid data, output =Target$+ \times +9.5 \times 10^{e} - 06$ for All data are are shown in figure **??**.The comparison of target and output with error is shown in figure **??**.

Figure **??** shows the examination of all data for the given model in integer format by deep NN with 1 coefficient of regression being fitted well. The mean square error (MSE) is 2.6×10^{-09} and the root mean square error (RMSE) is 4.4×10^{-05}. The mean and variance errors are 7.1×10^{-07} and 4.48×10^{-05} in histogram format. The small error implies correctness of the obtained scheme. Figure **??** tested train data in integer form for the said model with regression 1, the MSE is 1.6×10^{-09} and RMSE is 4.2×10^{-05} while the mean error is -1.02×10^{-07} and variance error is 4.2×10^{-05} in the histogram plot. Figure **??** shows the graphical representation for valid data in integer form for the said model with regression is 1, the MSE is 2.8×10^{-09} and RMSE is 5.3×10^{-05} while the mean error is 3.3×10^{-06} and variance error is 5.3×10^{-05} in the histogram plot. Figure **??** shows test data in fractal-fractional format for the given model with regression is 1, the MSE is 2×10^{-09} and RMSE is 4.5×10^{-05} while the mean error is 2.0×10^{-06} and variance error is 4.5×10^{-05} in the histogram plot showing best accuracy.

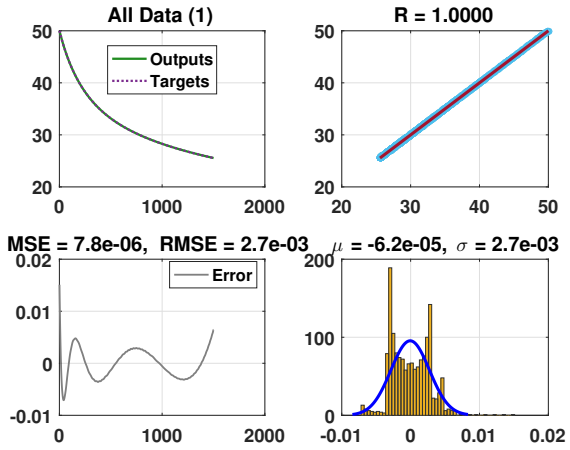

(a)

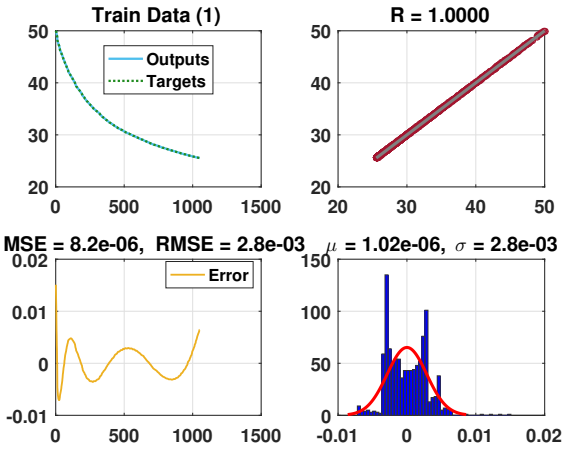

(b)

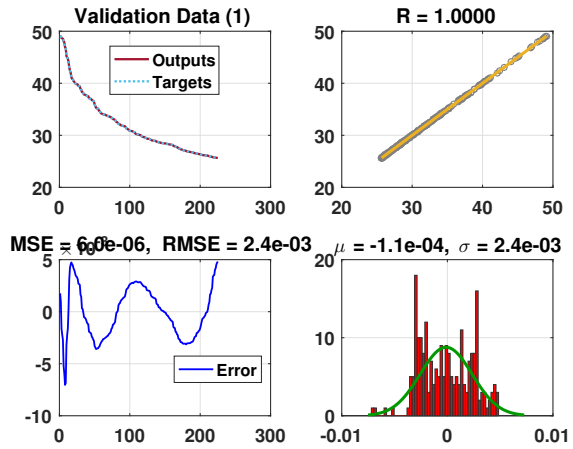

(c)

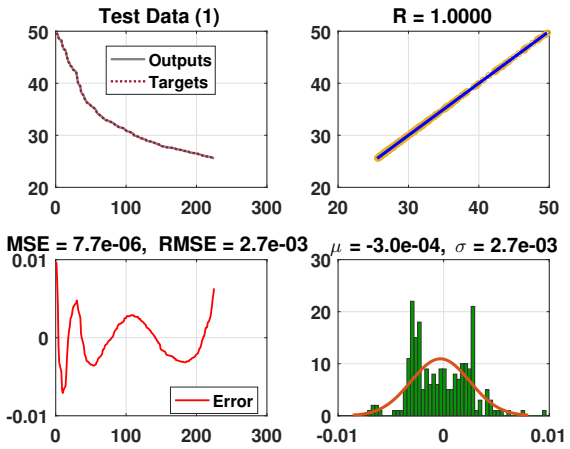

(d)

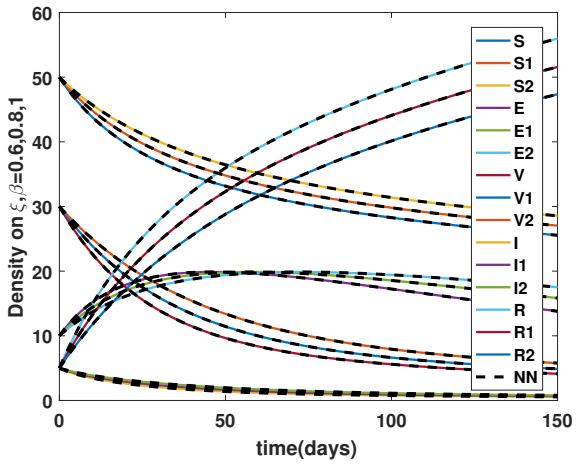

(e)

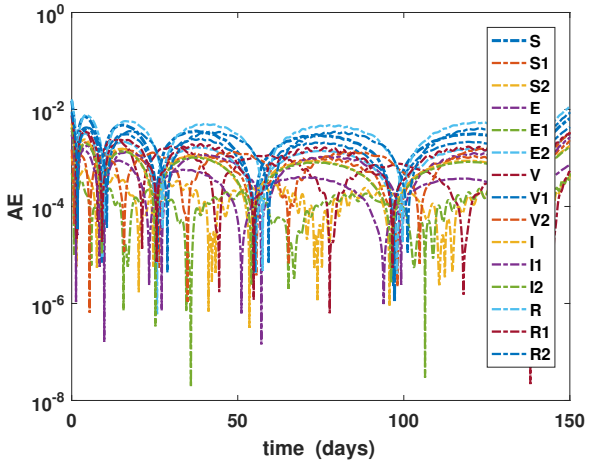

(f)

Fig. 3: Neural network dynamics of all the five compartments for (a) All data, (b) Train data, (c) Valid data, (d) Test data, (e) Comparison of ABM with NN, (f) Absolute error on three different fractal fractional orders.

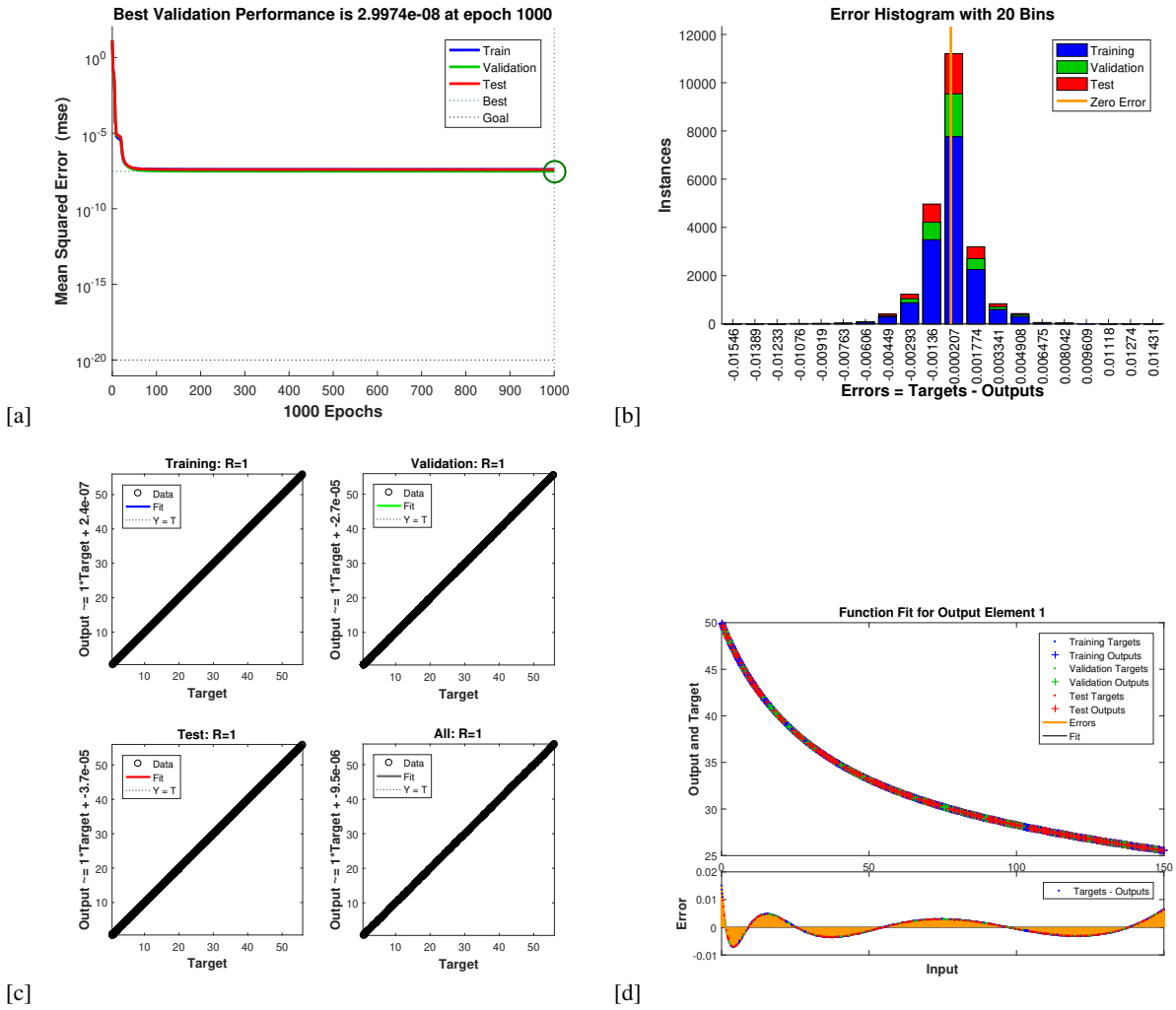

Fig. 4: Neural network performance of all the five compartments in (a) Histogram error in (b) regression for all data in (c) Curve Fitting of target and output with error in (d).

Furthermore the graphical representations of the performance for train, valid and test data for all five compartments in fractal integer format on 483 epoch is 9.43333×10^{-12} shown in figure **??**. Next the error of all compartments for 20 bins of train, valid and test data are given in figure **??**. The target for regression of data and fitting in the form of output =Target+ $\times$ +3.7 $\times$ 10^{e} −08 for train data, output =Target + $\times$ +9.5 $\times$ 10^{e} −07 for valid data, output =Target+ $\times$ +3.6 $\times$ 10^{e} −07 for All data are are shown in figure **??**. The comparison of target and output with error is shown in figure **??**. In about all cases they show very small error.

6 Conclusions

In this article, we adopted the framework of the fractal fractional-order derivatives of Caputo to investigate a complex geometrical model of a conjunctivitis virus for eyes infection having fractal dimension and fractional order. We conducted a theoretical analysis that includes stability results and existence theorems. Fixed point theory has been employed for qualitative analysis to ensure that the problem has at least one solution. We also explore the stability of the model using the Ulam-Hyers approach. Additionally, we developed an algorithm based on the fractional Adams-Bashforth method to provide numerical solutions having the parameters for fractal and fractional order for the extra choice of selection of numerical values lying between 0 and 1. The said dynamics are plotted against time 150 days with the inclusion of vaccination class, the eye infection is recovered and controlled very quickly. The recovery is achieved quickly and high

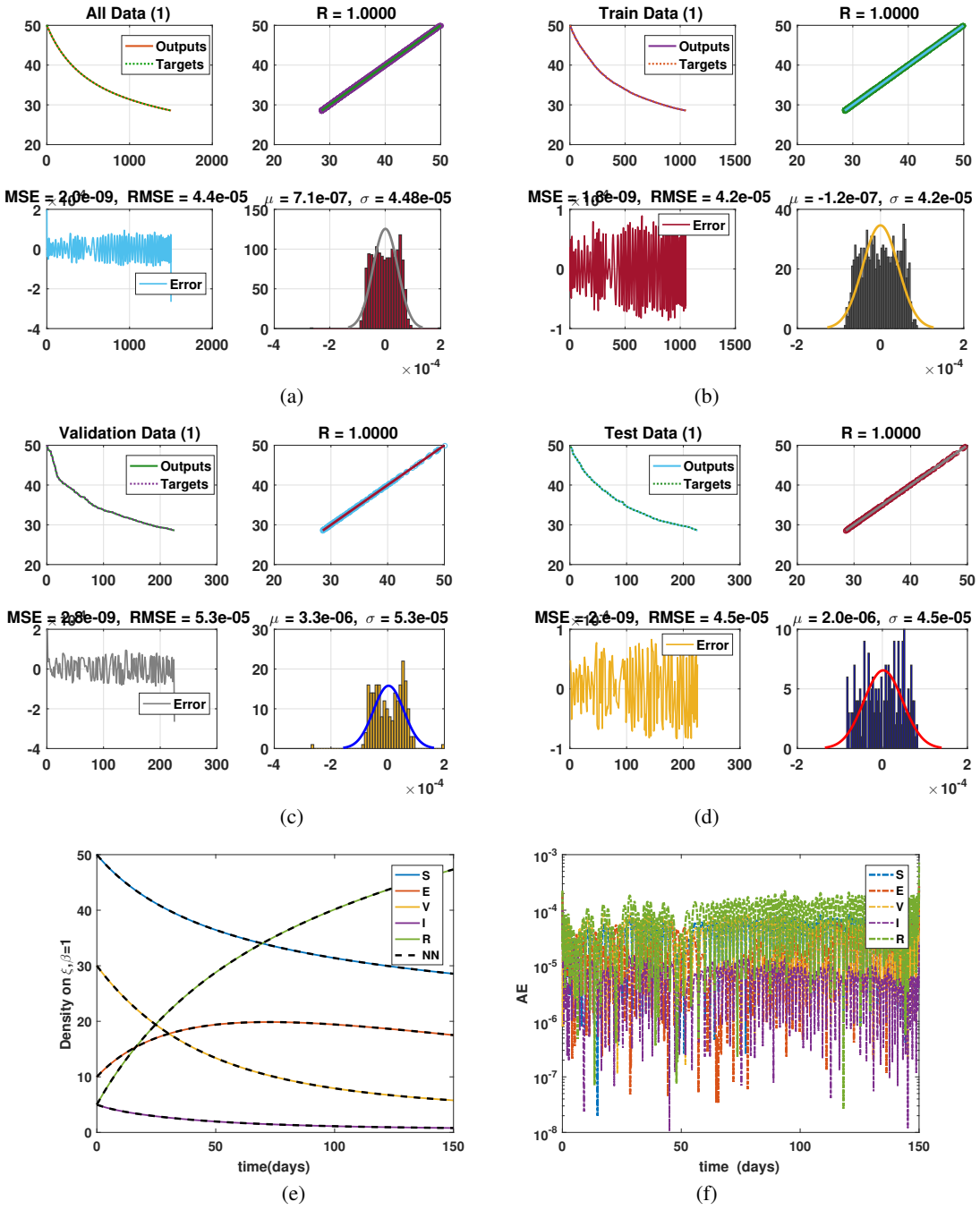

Fig. 5: Neural network dynamics of all the five compartments for (a) All data, (b) Train data, (c) Valid data, (d) Test data, (e) Comparison of ABM with NN, (f) Absolute error on three different fractal fractional orders.

on small fractal fractional orders and with low infection. The required dynamics are also tested in real stochastic format of neural network of hidden layers for all, train, valid and test data showing very less error of ranges $10^{-09} - 10^{-07}$ which pointed to the correctness of the obtained scheme. All the error including means square, root mean square, absolute, target vs output and ABS vs NN are drawn with very less values. Such kind of analysis may also be used for the future predictions of eye infections in the society and well be very helpful for the policy makers for this disease.

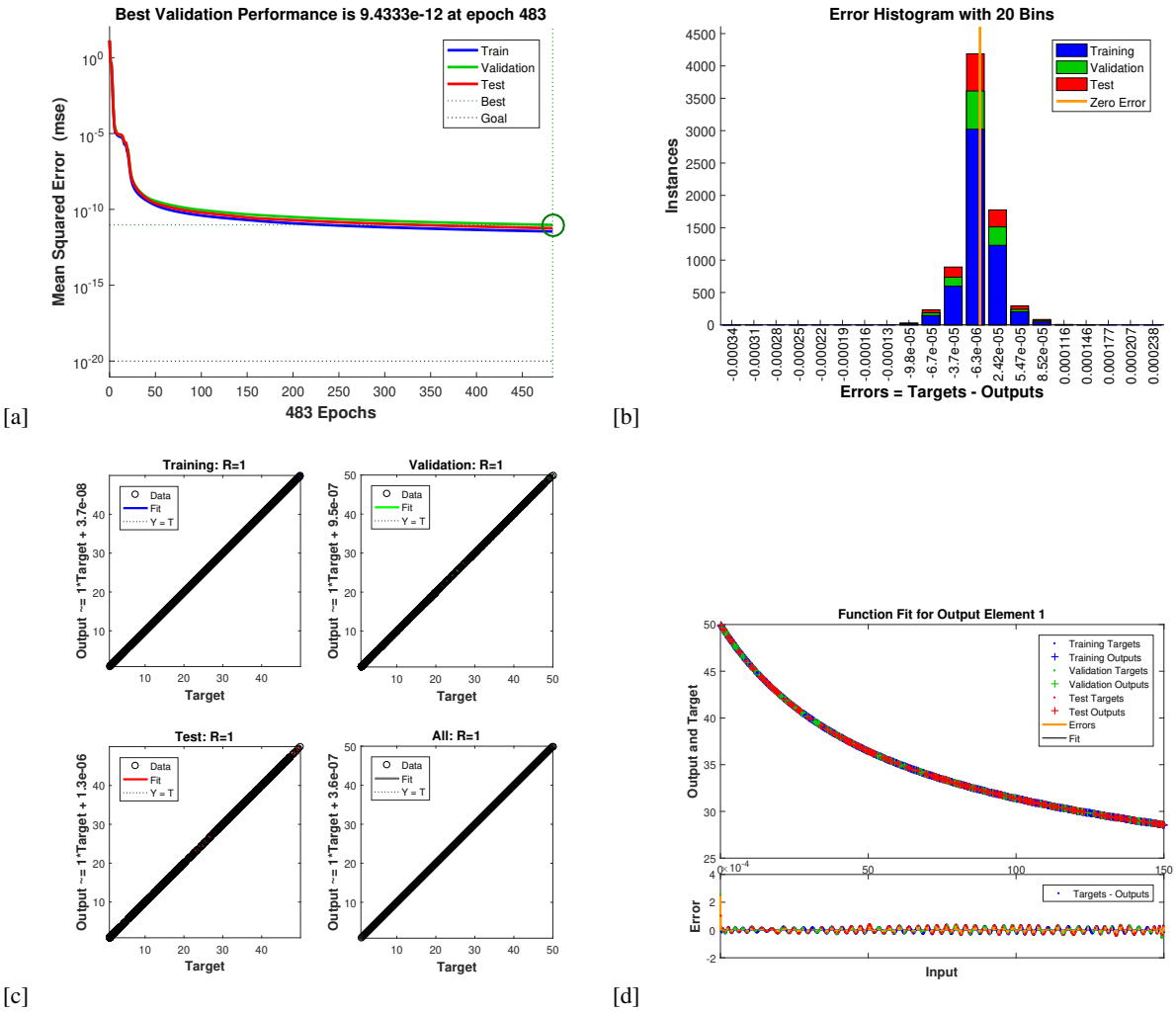

Fig. 6: Neural network performance of all the five compartments in (a) Histogram error in (b) regression for all data in (c) Curve Fitting of target and output with error in (d).

Declarations

Conflict of interest

The authors declare that they have no conflict of interest.

Data availability

No data was used or generated in the paper.

Authorship contribution statement

The authors have equally contributed to the paper. All authors read and approved the final manuscript.

Acknowledgment

The authors extend their appreciation to Prince Sattam bin Abdulaziz University for funding this research work through the project number (PSAU/2025/03/34359).

References

[1] Chou, C. S., & Friedman, A. (2016). *Introduction to mathematical biology*. In *Springer undergraduate texts in mathematics and technology* (Vol. 1, pp. 1–10). Springer International Publishing.

[2] Yeargers, E. K., Herod, J. V., & Shonkweiler, R. W. (2013). *An introduction to the mathematics of biology: With computer algebra models*. Springer Science & Business Media.

[3] Ghazali, O., Chua, K. B., Ng, K. P., Hooi, P. S., Pallansch, M. A., Oberste, M. S., & Others. (2003). *An outbreak of acute haemorrhagic conjunctivitis in Melaka*. *Singapore Medical Journal, 44*(10), 511–516.
[4] Kyere, S. N., Boateng, F. A., Hoggar, G. F., & Jonathan, P. (2018). *Optimal control model of haemorrhagic conjunctivitis disease*. *Advances in Computer Science*, *1*(2), 108.
[5] Centers for Disease Control and Prevention (CDC). (n.d.). *Conjunctivitis (pink eye)*. U.S. Department of Health & Human Services. https://www.cdc.gov
[6] Fehily, S. R., Cross, G. B., & Fuller, A. J. (2015). *Bilateral conjunctivitis in a returned traveller*. *PLoS Neglected Tropical Diseases, 9*(1), e0003351. https://doi.org/10.1371/journal.pntd.0003351
[7] Elliot, R. H. (1925). *Conjunctivitis in the tropics*. *British Medical Journal, 1*(3340), 12.
[8] Kimberlin, D. W. (Ed.). (2018). *Red Book: 2018–2021 report of the Committee on Infectious Diseases* (31st ed., pp. 152). American Academy of Pediatrics.
[9] Sangsawang, S., Tanutpanit, T., Mumtong, W., & Pongsumpun, P. (2012). Local stability analysis of mathematical model for hemorrhagic conjunctivitis disease. *Current Applied Science and Technology*, *12*(2), 189–197.
[10] Chansaenroj, J., Vongpunsawad, S., Puenpa, J., Theamboonlers, A., Vuthitanachot, V., Chattakul, P., … & Poovorawan, Y. (2015). Epidemic outbreak of acute haemorrhagic conjunctivitis caused by coxsackievirus A24 in Thailand, 2014. *Epidemiology & Infection, 143*(14), 3087–3093.
[11] Rihan, A., Sheek-Hussein, M., Tridane, A., & Yafia, R. (2017). Dynamics of Hepatitis C virus infection: Mathematical modeling and parameter estimation. *Mathematical Modelling of Natural Phenomena, 12*(5), 33–47.https://doi.org/10.1051/mmnp/201712504
[12] Khan, T., Rihan, F. A., & Ahmad, H. (2023). Modelling the dynamics of acute and chronic Hepatitis B with optimal control. *Scientific Reports, 13*(1), 14980. https://doi.org/10.1038/s41598-023-41925-6
[13] Rihan, F. A., & Udhayakumar, K. (2023). Fractional order delay differential model of a tumor-immune system with vaccine efficacy: Stability, bifurcation and control. *Chaos, Solitons & Fractals, 173*, 113670. https://doi.org/10.1016/j.chaos.2023.113670
[14] Ahmad, A., Kulachi, M. O., Farman, M., Junjua, M. U. D., Riaz, M. B., & Riaz, S. (2024). Mathematical modeling and control of lung cancer with IL-2 cytokine and anti-PD-L1 inhibitor effects for low immune individuals. *PLOS ONE, 19*(3), e0299560.https://doi.org/10.1371/journal.pone.0299560
[15] Alsaud, H., Kulachi, M. O., Ahmad, A., & Taimoor, M. (2024). Investigation of SEIR model with vaccinated effects using sustainable fractional approach for low immune individuals. *AIMS Mathematics, 9*(4), 10208–10234.https://doi.org/10.3934/math.2024393.
[16] Shah, M., & Abdeljawad, T. (2022). Study of a mathematical model of COVID-19 outbreak using some advanced analysis. In *Waves in Random and Complex Media*, 1–18.
[17] Ahmad, I., Shah, K., ur Rahman, G., & Baleanu, D. (2020). Stability analysis for a nonlinear coupled system of fractional hybrid delay differential equations. *Mathematical Methods in the Applied Sciences, 43*(15), 8669–8682. https://doi.org/10.1002/mma.6446
[18] Khan, A., Khan, Z. A., Abdeljawad, T., & Khan, H. (2022). Analytical analysis of fractional-order sequential hybrid system with numerical application. *Advances in Continuous and Discrete Models, 2022*(1), 12. https://doi.org/10.1186/s13662-021-03697-3
[19] Khan, H., Alzabut, J., & Gulzar, H. (2023). Existence of solutions for hybrid modified ABC-fractional differential equations with p-Laplacian operator and an application to a waterborne disease model. *Alexandria Engineering Journal, 70*, 665–672. https://doi.org/10.1016/j.aej.2022.08.005
[20] Khan, H., Alzabut, J., Tunç, O., & Kaabar, M. K. (2023). A fractal-fractional COVID-19 model with a negative impact of quarantine on the diabetic patients. *Results in Control and Optimization, 10*, 100199. https://doi.org/10.1016/j.rico.2023.100199
[21] Hussain, S., Madi, E. N., Khan, H., Etemad, S., Rezapour, S., Sitthiwirattham, T., & Patanarapeelert, N. (2021). Investigation of the stochastic modeling of COVID-19 with environmental noise from the analytical and numerical point of view. *Mathematics, 9*(23), 3122. https://doi.org/10.3390/math9233122
[22] Hussain, S., Tunç, O., ur Rahman, G., Khan, H., and Nadia, E. (2023). Mathematical analysis of stochastic epidemic model of MERS-corona & application of ergodic theory. *Mathematics and Computers in Simulation*, **207**, 130–150.
[23] Khan, H., Ahmed, S., Alzabut, J., & Azar, A. T. (2023). A generalized coupled system of fractional differential equations with application to finite time sliding mode control for Leukemia therapy. *Chaos, Solitons & Fractals, 174*, 113901. https://doi.org/10.1016/j.chaos.2023.113901
[24] Khan, Z. A., Khan, A., Abdeljawad, T., & Khan, H. (2022). Computational analysis of fractional order imperfect testing infection disease model. *Fractals, 30*(5), 2240169. https://doi.org/10.1142/S0218348X22401691
[25] Sharma, V. S., Singh, A., & Malik, P. (2024). Bifurcation patterns in a discrete predator–prey model incorporating ratio-dependent functional response and prey harvesting. *Qualitative Theory of Dynamical Systems, 23*(2), 74.
[26] Sharma, V. S., Singh, A., Elsonbaty, A. S., & Elsadany, A. A. (2023). Codimension-one and -two bifurcation analysis of a discrete-time prey–predator model. *International Journal of Dynamics and Control, 11*(6), 2691–2705.
[27] Sharma, V. S., & Singh, A. (2023). Strong resonance bifurcations and state feedback control in a discrete prey–predator model with harvesting effect. *Qualitative Theory of Dynamical Systems, 22*(3), 109.
[28] Singh, A., & Sharma, V. S. (2023). Bifurcations and chaos control in a discrete-time prey–predator model with Holling type-II functional response and prey refuge. *Journal of Computational and Applied Mathematics, 418*, 114666.
[29] Sangsawang, S., Tanutpanit, T., Mumtong, W., & Pongsumpun, P. (2012). Local stability analysis of mathematical model for hemorrhagic conjunctivitis disease. *Current Applied Science and Technology, 12*(2), 189–197.

[30] Ghazali, O., Chua, K. B., Ng, K. P., Hooi, P. S., Pallansch, M. A., Oberste, M. S., et al. (2003). An outbreak of acute haemorrhagic conjunctivitis in Melaka, Malaysia. *Singapore Medical Journal, 44*(10), 511–516.
[31] Chansaenroj, J., Vongpunsawad, S., Puenpa, J., Theamboonlers, A., Vuthitanachot, V., Chattakul, P., et al. (2015). Epidemic outbreak of acute haemorrhagic conjunctivitis caused by coxsackievirus A24 in Thailand, 2014. *Epidemiology and Infection, 143*(14), 3087–3093.
[32] Chowell, G., Shim, E., Brauer, F., Diaz-Duenas, P., Hyman, J. M., & Castillo-Chavez, C. (2006). Modelling the transmission dynamics of acute haemorrhagic conjunctivitis: Application to the 2003 outbreak in Mexico. *Statistical Methods in Medical Research, 25*(11), 1840–1857.
[33] Suksawat, S., & Naowarat, S. (2014). Effect of rainfall on the transmission model of conjunctivitis. *Advances in Environmental Biology, 8*(14), 99–104.
[34] Unyong, B., & Naowarat, S. (2014). Stability analysis of conjunctivitis model with nonlinear incidence term. *Australian Journal of Basic and Applied Sciences, 8*(24), 52–58.
[35] Sangthongjeen, S., Sudchumnong, A., & Naowarat, S. (2015). Effect of educational campaign on transmission model of conjunctivitis. *Australian Journal of Basic and Applied Sciences, 9*(7), 811–815.
[36] Kulachi, M. O., Ahmad, A., Hincal, E., Ali, A. H., Farman, M., & Taimoor, M. (2024). Control of conjunctivitis virus with and without treatment measures: A bifurcation analysis. *Journal of King Saud University - Science*, 103273.
[37] Sangsawang, S., Tanutpanit, T., Mumtong, W., and Pongsumpun, P. (2012). Local stability analysis of mathematical model for hemorrhagic conjunctivitis disease. *Current Applied Science and Technology*, **12**(2), 189–197.
[38] Rahman, M. U., Arfan, M., Shah, Z., Kumam, P., & Shutaywi, M. (2021). Nonlinear fractional mathematical model of tuberculosis (TB) disease with incomplete treatment under Atangana-Baleanu derivative. *Alexandria Engineering Journal*, 60(3), 2845-2856.
[39] Duve, P., Charles, S., Munyakazi, J., Lühken, R., & Witbooi, P. (2024). A mathematical model for malaria disease dynamics with vaccination and infected immigrants. *Mathematical Biosciences and Engineering*, 21(1), 1082-1109.
[40] M. Toufika and A. Atangana, *New numerical approximation of fractional derivative with non-local and non-singular kernel: application to chaotic models*, The Eur. Phys. J. Plus **132** (2017), no. 10, 444
[41] S. Sangsawang, T. Tanutpanit, W. Mumtong and P. Pongsumpun, Local Stability Analysis of Mathematical Model for Hemorrhagic Conjunctivitis Disease, *KMITL Sci. Tech. J.* 12 (2) (2012) 189-197.